https://doi.org/10.5194/nhess-2020-345
Preprint. Discussion started: 11 December 2020

Natural Hazards and Earth System Sciences
Discussions

Windstorms in the Northeastern United States

Frederick W. Letson[1], Rebecca J. Barthelmie[2], Kevin I. Hodges[3] and Sara C. Pryor[1]

[1]Department of Earth and Atmospheric Sciences, Cornell University, Ithaca, New York, USA
[2]Sibley School of Mechanical and Aerospace Engineering, Cornell University, Ithaca, New York, USA
[3]Environmental System Science Centre, University of Reading, Reading, United Kingdom

Correspondence to: F. Letson (fl368@cornell.edu), S.C. Pryor (sp2279@cornell.edu)

Abstract. Windstorms are a major natural hazard in many countries. Windstorms during the last four decades in the U.S. Northeast are identified and characterized using the spatial extent of locally extreme wind speeds at 100 m height from the ERA5 reanalysis database. During all of the top 10 windstorms, wind speeds in excess of their local 99.9th percentile extend over at least one-third of land-based ERA5 grid cells in this high population density region of the U.S. Maximum sustained wind speeds during these windstorms range from 26 to over 43 ms^{-1}, with wind speed return periods exceeding 6.5 to 106 years (considering the top 5% of grid cells during each storm). The property damage associated with these storms (inflation adjusted to January 2020) is $24 million to over $29 billion. Two of these windstorms are linked to decaying tropical cyclones, three are Alberta Clippers and the remaining storms are Colorado Lows. Two of the ten re-intensified off the east coast leading to development of Nor'easters. These windstorms followed frequently observed cyclone tracks, but exhibit maximum intensities as measured using 700 hPa relative vorticity and mean sea level pressure that are five to ten times mean values for cyclones that followed similar tracks over this 40-year period. The time-evolution of wind speeds and concurrent precipitation for those windstorms that occurred after the year 2000 exhibit good agreement with in situ ground-based and remote sensing observations, plus storm damage reports, indicating that the ERA5 reanalysis data have a high degree of fidelity for large, damaging windstorms such as these. A larger pool of the top 50 largest windstorms exhibits evidence of serial clustering, but to a degree that is lower than comparable statistics from Europe.

1 Introduction

1.1 Hazardous wind phenomena

Hazardous wind phenomena span a range of scales from extra-tropical cyclones down to downburst and gust fronts associated with deep convection (Golden and Snow, 1991). Herein we focus on large-scale, long duration 'windstorms' associated with extratropical cyclones since they are likely to have the most profound societal impacts. These large-scale windstorms are a feature of the climate of North America and Europe and a major contributor to weather-related social vulnerability and insurance losses (Della-Marta et al., 2009;Feser et al., 2015;Hirsch et al., 2001;Changnon, 2009;Ulbrich et al., 2001;Haylock, 2011;Lukens et al., 2018;Marchigiani et al., 2013).

This analysis focusses on windstorms in the Northeastern region of the United States (U.S.) as defined in the National Climate Assessment (USGCRP, 2018) (Table 1). This region exhibits a very high prevalence of mid-latitude cyclone passages (Hodges et al., 2011;Ulbrich et al., 2009) and the associated extreme weather events (Bentley et al., 2019). It lies under a convergence zone of two prominent Northern Hemisphere cyclone tracks

https://doi.org/10.5194/nhess-2020-345
Preprint. Discussion started: 11 December 2020

Natural Hazards and Earth System Sciences Discussions

associated with cyclones that form or redevelop as a result of lee-cyclogenesis east of the Rocky Mountains (Lareau and Horel, 2012). The first is associated with extra-tropical cyclones that have their genesis in the lee of Rocky Mountains within/close to the U.S. state of Colorado and typically track towards the northeast (Colorado Lows, CL) (Bierly and Harrington, 1995;Hobbs et al., 1996). The second is characterized by cyclones that have their genesis in the lee of Rocky Mountains in/close to the Canadian province of Alberta and track eastwards across the Great Lakes (Alberta Clippers, AC). Previous research has found that these cyclones generally move southeastward from the lee of the Canadian Rockies toward or just north of Lake Superior (Fig. 1a) before progressing eastward into southeastern Canada or the northeastern United States, with less than 10% of the cases in the climatology tracking south of the Great Lakes (Thomas and Martin, 2007). The northeastern states are also impacted by decaying tropical cyclones (TC) that track north from the Gulf of Mexico or along the Atlantic coastline (Baldini et al., 2016;Varlas et al., 2019;Halverson and Rabenhorst, 2013). Consistent with recent research on the windstorm risk in Europe that found that although less than 1% of cyclones that impact Northern Europe are post tropical cyclones, these systems tend to be associated with higher 10-m wind speeds (Sainsbury et al., 2020). Tropical cyclones, such as Hurricane Sandy have been associated with large geophysical hazards in the Northeast (Halverson and Rabenhorst, 2013;Lackmann, 2015). This region also experiences episodic Nor'easters, extra-tropical cyclones that form or intensify off/along the U.S. east coast and exhibit either retrograde or northerly track resulting in a strong northeasterly flow over the Northeastern states (Hirsch et al., 2001;Zielinski, 2002).

Table 1. Summary of the states that comprise the Northeastern region as defined by the National Climate Assessment.(USGCRP, 2018). State abbreviations and population from the 2010 U.S. Census are also given (Census, 2019).

Name	Abbreviation	2010 Population
United States	US	308,745,538
Northeastern Region	NE	64,443,443
Connecticut	CT	3,574,097
Delaware	DE	897,934
District of Columbia	DC	601,723
Maine	ME	1,328,361
Maryland	MD	5,773,552
Massachusetts	MA	6,547,629
New Hampshire	NH	1,316,470
New Jersey	NJ	8,791,894
New York	NY	19,378,102
Pennsylvania	PA	12,702,379
Rhode Island	RI	1,052,567
Vermont	VT	625,741
West Virginia	WV	1,852,994

There is evidence that intense winter wind speeds in the mid-latitudes have increased since 1950, due in part to increased frequency of intense extra-tropical cyclones (Ma and Chang, 2017;Vose et al., 2014). While long-term trends such as this from reanalysis products are subject to the effects of changing data assimilation (Bloomfield et al., 2018;Befort et al., 2016;Bengtsson et al., 2004), the 56 member twentieth century reanalysis exhibits a positive trend in the 98th percentile wind speed over parts of the U.S. including the Northeastern states that are the focus of the current research (Brönnimann et al., 2012) (Fig. 1, Table 1).

https://doi.org/10.5194/nhess-2020-345
Preprint. Discussion started: 11 December 2020

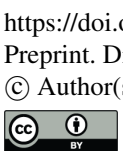

Natural Hazards and Earth System Sciences
Discussions
Open Access
EGU

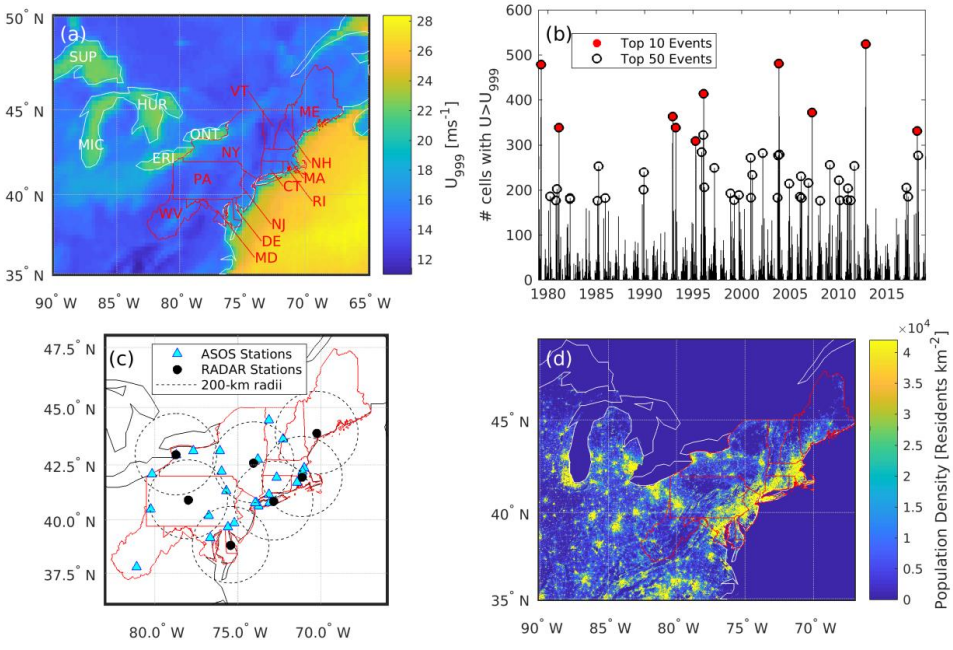

Figure 1. (a) 99.9th percentile wind speed (U_{999}) from ERA5 for each grid cell in the Northeastern U.S. derived using hourly wind speeds at 100 m a.g.l. during 1979-2018. Borders of the 12 Northeastern states are shown in red. The Great Lakes are each labelled in white, with the first three letters of their names: Superior (SUP), Michigan (MIC), Huron (HUR), Erie (ERI) and Ontario (ONT). (b) Time series of the number of ERA5 grid cells over the Northeastern states that exceed their local U_{999} value (out of 924 cells). The 50 largest-magnitude events are circled in black, and the top ten events are marked in red. (c) Locations of the 24 ASOS stations and 7 RADAR stations used for validation of ERA5 wind speed and precipitation values. The dotted circles show the area with 200-km radius from each RADAR station (d) Population density of the Northeast at a spatial resolution of 30 arc-seconds (~1 km; data from the 2010 U.S. Census).

1.2 Socioeconomic consequences of windstorms

Economic losses associated with atmospheric hazards are substantial. Data from Munich Re indicate that annual 'weather related' losses at the global scale in 1997-2006 were US $45.1 billion (inflation adjusted to 2006 $) (Bouwer et al., 2007). In 2013, globally aggregated losses due to natural hazards were estimated at US$125 billion (Kreibich et al., 2014). Data from the contiguous U.S. indicate 168 "billion-dollar disaster events" linked to atmospheric phenomena during 1980-2013 (Smith and Matthews, 2015). In the U.S., three-quarters of total damages from natural hazards derive from hurricanes, flooding, and severe winter storms (including windstorms) (Gall et al., 2011). There is also evidence of a trend towards increasing economic impact from natural hazards within the U.S. even after adjusting for inflation. According to one report; 'Nationwide, annual losses rose from $4.7 billion in the 1960s to $6.7 billion in the 1970s, $7.6 billion in the 1980s, $14.8 billion in the 1990s, and $23.6 billion in the 2000s' due to a combination of more frequent disasters, disasters of larger scale and changes in societal resilience (Gall et al., 2011).

Here we focus on the Northeastern U.S. states (Fig. 1a, Table 1) because this region experiences a relatively high frequency of damaging storms, in particular during the cold season (Hirsch et al., 2001), and exhibits relatively high exposure due to both the large number of (i) highly populated, high-density urban areas (Fig. 1d (SEDAC, 2020;Census, 2019)) and (ii) high-value (insured) assets. For example, New York state ranks tenth of fifty U.S.

https://doi.org/10.5194/nhess-2020-345
Preprint. Discussion started: 11 December 2020


Natural Hazards and Earth System Sciences
Discussions

states in total direct economic losses related to natural hazards, with estimated losses of $12.54 billion in 2009$ between 1960 to 2009 (Gall et al., 2011).

Windstorms present a hazard to the built environment, transportation, especially to aviation (Young and Kristensen, 1992), and multi-energy systems including the electric grid (Bao et al., 2020;Wanik et al., 2015). In 2016 the annual cost of grid disruptions within the U.S. were estimated to range from approximately $28 billion to $209 billion (Mills and Jones, 2016). Composite events characterized by the co-occurrence of ice accumulation and wind are particularly hazardous to the built environment, aviation and energy infrastructure (Sinh et al., 2016;Jeong et al., 2019). For example, in the 1998 Northeastern ice storm ice deposition combined with high winds led to the toppling of 1,000 transmission towers, loss of power to 5 million people, and 840,000 insurance claims valued at $1.2 billion (Mills and Jones, 2016).

1.3 Objectives of this research

This research is inspired by and is conceptually analogous to development of the XWS (eXtreme WindStorms) catalogue of storm tracks and wind-gust footprints for 50 of the most extreme European winter windstorms (Roberts et al., 2014). Specific goals of the research reported herein are to:

1) Present a new method for identifying and physically characterizing severe windstorms. This method is applied to forty-years of hourly output from the ERA5 reanalysis to extract the 10 most intense windstorms over the U.S. Northeastern states and describe them in terms of their location, spatial extent, duration, and severity. We further evaluate the degree to which these windstorms are composite extreme events, wherein high wind speeds co-occur with extreme or hazardous precipitation.
2) Verify aspects of the windstorms as characterized based on ERA5 reanalysis output using wind speed observations from sonic anemometers and precipitation characteristics from RADAR and in situ rain gauges, plus storm damage reports.
3) Contextualize these windstorms in the long-term cyclone climatology. Specifically, we track each windstorm over time and space using two indices of intensity derived from mean-surface pressure and relative vorticity and contextualize these events in the cyclone climatology for 1979-2018.
4) Evaluate these windstorms in terms of the return periods of extreme wind speeds derived using the Gumbel distribution applied using annual maximum wind speeds for 1979-2018.

This research is a part of the HyperFACETS project which uses a storyline-based analysis framework. Storylines are “physically self-consistent unfolding of past events, or of plausible future events or pathways” (Shepherd et al., 2018) and provide a method of framing a research inquiry in terms of three elements: A geographic region, an event, and a set of process drivers for that event.

2 Data and Methods

2.1 ERA5 reanalysis

Attempts to identify and characterize windstorms from a geophysical perspective have historically been hampered by limited data availability and/or quality from geospatially inhomogeneous observing networks. Further, time series from in situ wind measurement networks exhibit substantial inhomogeneities due to factors such as station relocations, instrumentation changes, changes in conditions around individual measurement stations, changes in

https://doi.org/10.5194/nhess-2020-345
Preprint. Discussion started: 11 December 2020


Natural Hazards and Earth System Sciences
Discussions

measurement frequencies and/or integration periods (Pryor et al., 2009;Wan et al., 2010). Thus, herein we employ once hourly wind speeds from the ERA5 reanalysis. The wind speeds are for a height of 100-m a.g.l. at the model time step of 20 minutes and a spatial resolution of 0.25°×0.25°. This study focuses on windstorms within a study domain that extends from 35 to 50°N and 65 to 90°W (Fig. 1a). The events are defined using data from the 924 ERA5 land-dominated grid cells over the twelve Northeastern states (two-letter abbreviations given in Table 1).

The ERA5 reanalysis is derived using an unprecedented suite of assimilated in situ and remote sensing observations (Hersbach et al., 2020) and exhibits relatively high fidelity for wind speeds (Kalverla et al., 2020;Olauson, 2018;Kalverla et al., 2019;Pryor et al., 2020;Jourdier, 2020;Ramon et al., 2019). However, it is important to acknowledge that wind parameters from any model do not fully reflect all scales of flow variability (Skamarock, 2004) and underestimate extreme wind speeds (Larsén et al., 2012), particularly in areas with high orographic complexity and or varying surface roughness length. Here we use wind speeds at 100-m because flow at this height is less likely to be impacted by sub-grid scale heterogeneity in surface roughness length and uncertainties induced by unresolved sub-grid scale variability. Near-surface wind speeds are strongly coupled to wind speeds at 100-m (i.e. within the PBL) but wind speeds at 100-m are less strongly impacted by inaccuracies and/or uncertainty in surface roughness length (z_0) (Minola et al., 2020;Nelli et al., 2020). Applying an uncertainty of a factor of two to z_0 can lead to mean differences of up to 0.75 ms^{-1} for near-surface (40 to 150 m a.g.l.) wind speeds (Dörenkämper et al., 2020). Further, the scale of events we seek to characterize are regional rather than local scale, and are necessarily driven by winds aloft.

Cyclone tracking and intensity estimates presented herein employ three-hourly mean sea level pressure (MSLP) and relative vorticity at 700 hPa (RV) fields from ERA5. Previous research has indicated relatively good consistency between cyclone climatologies derived using ERA5 and other recent reanalyses (Gramcianinov et al., 2020;Sainsbury et al., 2020). RV values at 700 hPa are used rather than 850 hPa as in the XWS European analysis due to the presence of high elevation areas in U.S. cyclone source regions. Further, the three-hourly fields from ERA5 used herein are direct products of the reanalysis, whereas the 3-hourly values used in XWS were based on 6-hourly ERA Interim reanalyses combined with ERA Interim forecast values for the intervening time steps (Roberts et al., 2014).

Compound events, windstorms which exhibit a co-occurrence of extreme precipitation and/or freezing rain with high winds, are associated with amplified risk (Zscheischler et al., 2018;Sadegh et al., 2018). Precipitation intensity and hydrometeor class from ERA5 are used to identify to what degree each of the ten storms are compound events. The hydrometeor classes reported by ERA5 are; rain, mixed rain and snow, wet snow, dry snow, freezing rain, and ice pellets and are differentiated based largely on the temperature structure in the reanalysis model (https://confluence.ecmwf.int/display/FUG/9.7+Precipitation+Types). Prior analyses of ERA5 precipitation values have indicated skill relative to in situ observations and gridded data sets over the U.S. (Tarek et al., 2020;Sun and Liang, 2020).

2.2 Observational data

Wind speeds and precipitation characteristics during the windstorms are identified using ERA5 and are validated using in situ measurements from 24 National Weather Service (NWS) Automated Surface Observation System (ASOS) stations and seven NWS RADARs (Fig. 1c). Since major upgrades to the NWS systems were conducted in 2000, this evaluation is focused on windstorms that occurred after that year. Five minute measurements of in

https://doi.org/10.5194/nhess-2020-345
Preprint. Discussion started: 11 December 2020


Natural Hazards and Earth System Sciences
Discussions

situ wind speeds at 10-m a.g.l. used in this evaluation derive from ice-free two-dimensional sonic anemometers (Schmitt IV, 2009), while the in situ observations of precipitation intensity reported from the ASOS network derive from heated tipping-bucket rain gauges (Tokay et al., 2010). In the absence of widespread in-situ wind speed observations from tall towers (which would be more comparable to the 100-m wind speeds from ERA5), these 10-m wind speed observations represent the best available validation data set for the occurrence of high winds throughout the Northeast states. NWS protocols document accumulated precipitation since the last hour, sampled every minute and reported every five minutes (Nadolski, 1998). For the current comparison to ERA5, these are averaged to generate hourly rainfall rates.

Precipitation rates from seven NWS dual polarization RADAR (Kitzmiller et al., 2013) are used to provide an areally-averaged comparison of ERA5 (Fig. 1c). NWS RADAR precipitation products are the product of extensive development efforts (Cunha et al., 2015;Villarini and Krajewski, 2010;Straka et al., 2000) and have been employed in a wide array of applications (Letson et al., 2020;Seo et al., 2015;Krajewski and Smith, 2002). Precipitation intensity rates derived from RADAR reflectivity are reported in 41,400 cells using 1° azimuth angle and a range resolution of 2 km. In the current work, precipitation rates within 200 km of each RADAR are averaged in time to match the hourly resolution of ERA5 precipitation and interpolated in space to the 0.25°×0.25° ERA5 grid. For comparison with ERA5, mean precipitation rates in each hour of the windstorm are computed from ERA5, ASOS and RADAR over the land areas of Northeastern states that are within 200 km of the 7 RADAR stations used herein (Fig. 1c).

2.3 NOAA Storm Events Database

The U.S. National Oceanic and Atmospheric Administration (NOAA) provides detailed information on "the occurrence of storms and other significant weather phenomena having sufficient intensity to cause loss of life, injuries, significant property damage, and/or disruption to commerce" at the county level in the NOAA Storm Events Database (https://www.ncdc.noaa.gov/stormevents/). These records are subject to some inhomogeneities associated with digitization of transcripts prior to 1993, and standardized into 48 event types in 2013 (https://www.ncdc.noaa.gov/stormevents/details.jsp?type=collection) but are compiled from a range of county, state and federal agencies in addition to the NWS. Like all hazard loss datasets they are subject to reporting inaccuracies and inconsistencies (Gall et al., 2009), but they represent a long and relatively consistent record, and are widely used (Young et al., 2017;Konisky et al., 2016). Damage and mortality estimates from this dataset to provide an estimate of the impact of each windstorm, with the caveat that population density and hence the potential for loss of life and damage vary markedly between U.S. counties (Fig. 1d).

2.4 Method used to characterize windstorms

A range of different techniques have been developed and applied to identify and characterize atmospheric hazards including extreme windstorms. Some rely on an assessment of the severity of the events such as insured losses or human mortality/morbidity, others prescribe a level of rarity (i.e. are probabilistic), while others prescribe a level of intensity (i.e. the occurrence of extreme values of some physical phenomena) (Stephenson, 2008). Here we employ a methodology based on the intensity and spatial extent of extreme wind speeds. This approach is conceptually similar to storm severity indices derived from European work based on the maximum 925 hPa wind speed within a 3° radius of the vorticity maximum and the area over which wind speeds at that height exceed 25

https://doi.org/10.5194/nhess-2020-345
Preprint. Discussion started: 11 December 2020


Natural Hazards and Earth System Sciences
Discussions

ms^{-1} (Roberts et al., 2014;Della-Marta et al., 2009). It also draws from earlier work that used an index defined as the product of the cube of the maximum observed wind speed over land, the areas impacted by damaging winds (> 25.7 ms^{-1}) and the duration of damaging winds (Lamb, 1991).

This analysis employs hourly wind speeds at 100-m a.g.l. for 1979-2018 in all 924 land-dominated grid cells over the Northeastern states. The methodology applied to identify and characterize the ten largest windstorms does not employ an absolute threshold of wind speed, but rather exceedance of locally determined thresholds defined by the 99.9th percentile wind speed value (U_{999}). A local U_{999} threshold is used, rather than an absolute wind speed threshold in ms^{-1}, in part because storms affecting urban areas, which may not be prone to high wind speeds, are especially damaging to infrastructure. While lower percentile thresholds have been used in previous work (Walz et al., 2017;Klawa and Ulbrich, 2003), use of the 99.9th percentile wind speed value is appropriate for identifying the truly extraordinary conditions we seek to characterize and is robust when applied to very long datasets with very large sample sizes. Use of locally determined thresholds also enables direct comparison of the spatial scale and intensity of windstorms derived using the ERA5 data at 100 m a.g.l. and near-surface wind speed observations from 10 m a.g.l.. Exceedance of the local 99.9th percentile wind speed value (U_{999}) value is considered in both cases based on the ~20 year record from each ASOS station and the 40 years of ERA5 data, and comparisons are made at an hourly resolution by averaging all ASOS wind speeds within a given hour.

As shown in Fig. 1a, there is marked spatial variability in the 99.9th percentile wind speed (i.e. the wind speed exceeded on slightly over 3500 hours during the forty-year period). U_{999} ranges from over 28 ms^{-1} over the Atlantic Ocean down to 12 ms^{-1} over some land grid cells due to the higher surface roughness and topographic drag. Windstorms are identified as periods when the largest number of ERA5 grid cells exceed their local (ERA5 grid cell specific) 99.9th percentile wind speed value ($U>U_{999}$). A further restriction is applied in that no event may be within 14 days of any other, to avoid double-counting of any individual storm (Fig. 1b, Table 2).

The peak hour of $U>U_{999}$ coverage within the Northeast states for each of the ten most intense storms is referred to herein as the peak windstorm time (t_p), and the 97 hours (±48 hours) surrounding that time are referred to as the storm period. For each hour of each storm period a high-wind centroid is identified using the mean latitude and longitude of all grid cells where $U>U_{999}$.

Precipitation associated with each of the ten most intense windstorms is also evaluated using ERA5 precipitation totals and types. The analysis of precipitation centers on a 24-hour period centered on the peak windstorm time (t_p). Precipitation statistics including 24-hour total precipitation, hourly precipitation rates, and the frequency of each precipitation type is characterized for all land grid cells in Northeastern states that exceed their local U_{999} value at any point in this 24-hour period.

Research from Europe indicate evidence of serial clustering of windstorms (Walz et al., 2018). Although our focus is primarily on the ten most intense and extensive windstorms, a larger sample of 50 events is extracted using the methodology described above but relaxing the temporal separation from 14 to 2 days, to examine the degree to which spatially extensive windstorms as manifest in ERA5 are serially clustered (Fig. 1b). This analysis employs a Poisson distribution fit to these 50 events and the dispersion index (D) of (Mailier et al., 2006):

$$D = \frac{\sigma^2}{\mu} - 1 \quad (1)$$

Where σ^2 and μ are the variance and mean of the distribution, which for a Poisson distributed random variable are equal (Wilks, 2011). D > 0 indicates the presence of temporal clustering. The significance of D is evaluated using a bootstrapping analysis in which 10,000 samples are drawn with replacement and the dispersion index is

https://doi.org/10.5194/nhess-2020-345
Preprint. Discussion started: 11 December 2020


Natural Hazards and Earth System Sciences
Discussions

calculated for each, similar to a method used in (Pinto et al., 2016).

2.5 Development of a cyclone climatology

A cyclone detection and tracking algorithm (Hodges et al., 2011) is applied to 3-hourly ERA5 MSLP and 700hPa RV global fields that have been subjected to T42 spectral filtering for RV (corresponding to a 310-km resolution at the equator) and T63 filtering for MSLP (210 km at the equator) with the large scale background removed for total wavenumbers ≤ 5. These spectral filters are designed to restrict detection to tropical and mid-latitude cyclones (Hoskins and Hodges, 2002). The location and intensity of the cyclones are identified using the local maxima in RV and the minima (i.e. negative deviations) in MSLP. These are anomalies identified in the filtered fields, obtained from the spectral filtering which has the large-scale background removed for the tracking. RV cyclone intensities are shown in units of 10^{-5} s^{-1}, and MSLP intensity estimates are given in hPa. The cyclones are tracked by first initializing a set of tracks based on a nearest-neighbor method which are then refined by minimizing a cost function for track smoothness as in the XWS European analysis (Roberts et al., 2014). Cyclones only contribute to the climatology if they persist for ≥ eight time steps (24 hours). The cyclone detection algorithm is applied separately to MSLP and RV with the results being used to provide a qualitative assessment of the uncertainty in the cyclone tracks.

Tracks associated with each windstorm are identified by identifying the geographic centroid of ERA5 grid cells where U > U_{999} and secondly if the local maximum of MSLP (scaled by -1) and RV anomalies tracked into the Northeast study domain during the storm period. The date and location on which the cyclone associated with each windstorm are first identified by the tracking algorithm are used to identify the source area of each windstorm and the location and time at which the detection algorithm ceases to identify a cyclone are used to describe the end of the cyclone track. Subjective evaluation of the cyclone tracks associated with each windstorm are used to identify the type of cyclone associated with each windstorms; Alberta Clippers (AC), deep Colorado lows (CL), decaying tropical cyclones (TC) and nor'easters (NE).

Consistent with past research (Hirsch et al., 2001) all of the top-10 windstorms identified using the largest spatial extent of locally extreme wind speeds in the ERA5 data occur during cold season months (October to April). Thus, the cyclone track density used to contextualize the windstorms is restricted to only those months. This analysis further focusses solely on cyclones that track into the Northeastern domain. These restrictions allow direct evaluation of the degree to which the windstorms are typical of the prevailing cyclone climatology.

2.6 Calculation of long-term period wind speeds

Peak wind speeds (U_{peak}) during each of the windstorms are expressed in terms of their return period (*RP* in years) to provide a metric of the degree to which these events are exceptional. These statistics are computed for each ERA5 grid cell by fitting a double exponential (Gumbel) distribution to annual maximum wind speeds (U_{max}) (Mann et al., 1998):

$$P(U_{max}; \alpha, \beta) = e^{-e^{(U_{max}-\alpha)/\beta}} \quad (2)$$

Where the distribution parameters α and β are derived using maximum likelihood estimation. The U_{peak} estimates for each ERA5 grid cell are then evaluated in terms of their return period (*RP* in years) using (Wilks, 2011;Pryor et al., 2012):

https://doi.org/10.5194/nhess-2020-345
Preprint. Discussion started: 11 December 2020

Natural Hazards and Earth System Sciences
Discussions

$$RP = \frac{1}{1-P(U_{peak})} \quad (3)$$

This method is similar to that used for grid-point-based wind speed return period calculations in previous work (Della-Marta et al., 2009), which resulted in return periods of 0.1 to 500 years when considering 200 prominent windstorms in Europe.

3 Results

3.1 Windstorm identification and characterization

The top-10 windstorms during 1979-2018 over the Northeastern states identified using the method described above are summarized in Table 2. During the peak hour (t_p) of each of these windstorms, 309 to 524 (33 to 56%) of the 924 ERA5 land-dominated grid cells exhibit $U>U_{999}$ (Table 2). For context, 10% of ERA5 grid cells co-exhibit $U>U_{999}$ in <1% of hours. The windstorms are not concentrated in any sub-period of the 40 years under consideration (1979-2018) and no individual year contained two of the top ten windstorms (Fig. 1b). Hence, in the following the windstorms are referred to below by their (unique) year of occurrence, and in all figures and tables results are displayed in decreasing order of windstorm magnitude as defined using spatial extent (Table 2). The maximum wind speed at 100 m a.g.l. in any ERA5 grid cell at the peak hour range from 25 to 41 ms^{-1}, while the maximum during the storm period range from 26 to 44 ms^{-1} (Table 2). These maximum wind speeds do not scale with the storm intensity as measured by the number of grid cells that exceed their local 99.9th percentile wind speeds (Table 2). For example, the windstorm during March 1993 was associated with the highest absolute wind speeds but was manifest in a relatively small number of ERA5 grid cells (Table 2).

Table 2. Summary of the top 10 windstorm events. The time of max coverage (t_p) shows the time and date with the greatest geographic extent of high wind speeds. # cells indicates the count of ERA5 grid cells with $U > U_{999}$ at t_p. The maximum precipitation accumulated in any Northeastern state land grid cell is given for in the 24 hours surrounding the storm peak. Property damage for the Northeastern states is the accumulation of information from the NOAA Storm Data accumulated over the duration of the period for which the associated cyclone (defined using RV) is evident. Inflation adjusted property damage are derived using inflation estimates from the U.S. Bureau of Statistics (bls.gov/data/inflation_calculator.htm)

Time of max coverage (t_p)	# cells $U>U_{999}$	Max U at t_p [ms^{-1}]	Max U during storm period [ms^{-1}]	Max 24-hour precip. [mm]	Property Damage [M$]	Property Damage [M$] Inflation adjusted to January 2020
10/30/2012 00:00	524	34.27	41.80	146.03	25,304	29,100
11/13/2003 20:00	481	26.04	29.95	39.02	1,119	1,600
4/6/1979 20:00	479	28.53	31.88	34.19	586	2,233
1/27/1996 15:00	414	25.76	30.81	60.64	1,298	2,181
4/16/2007 16:00	372	29.56	32.44	79.06	392	502
11/13/1992 3:00	363	25.53	28.34	54.01	42	79
2/11/1981 04:00	339	24.81	29.08	93.02	8	24
3/13/1993 21:00	339	40.95	43.15	84.33	34	62
3/2/2018 19:00	331	31.66	33.10	84.71	164	172
4/5/1995 20:00	309	24.21	26.29	19.19	225	389

All ten windstorms are associated with substantial damage reports within the Northeast states (Table 2, Fig. 2) and nine of the ten storms were responsible for deaths in the Northeast states (Fig. 2). There is not direct correspondence between the ranking of the windstorms in terms of the number of ERA5 grid cells with $U>U_{999}$, and the amount of damage and human mortality as reported in the NOAA Storm Data, but the four highest-magnitude windstorms (2012, 2003, 1979, and 1996) all have property damage totals above any of the other six windstorms (Table 2). Further, although NOAA Storm Data indicate only modest total economic costs associated

https://doi.org/10.5194/nhess-2020-345
Preprint. Discussion started: 11 December 2020

Natural Hazards and Earth System Sciences
Discussions

with property damage during the 1992 windstorm, there are reports of widespread damage in counties across much of the Northeast (Fig. 2). The lack of complete correspondence between the centroid of windstorms, as identified using the methodology presented here, and property damage in the NOAA dataset is likely due to: (i) Occurrence of localized extreme (damaging) winds that are manifest at scales below those represented in the ERA5 reanalysis (e.g. downbursts from embedded thunderstorms, sting jets and other mechanisms (Li et al., 2020;Clark and Gray, 2018)). (Hewson and Neu, 2015) suggest a grid resolution of 20 km or higher is required to fully capture damaging winds. (ii) Spatial variability in insured assets (e.g. (Nyce et al., 2015) and (Brown et al., 2015)). (iii) Possible inconsistences in storm-reporting practices across counties (See NOAA storm data publications for details: https://www.ncdc.noaa.gov/IPS/sd/sd.html). Nevertheless, although many factors dictate economic losses from windstorms, the Pearson correlation coefficient (r) between the number of grid cells with $U > U_{999}$ at t_p and inflation adjusted property damage exceeds 0.66, and r between the maximum wind speed and inflation adjusted property damage is 0.56. For a sample size of 10, using a t-test to evaluate significance (Wilks, 2011), these correlation coefficients differ from 0 at confidence levels of 95% and 90%, respectively. Thus, this geophysical intensity metric captures aspects of relevance to storm damage.

Several of the windstorms have been previously identified in independent analyses further confirming the reliability of the detection method. For example, Hurricane Sandy, the most intense windstorm in this analysis (Table 2), is a historic storm that moved parallel to the coast before making landfall in southern New Jersey on 29 October and caused $50 billion of damage (Lackmann, 2015). According to the ERA5 output at its peak, over 300,000 km^2 of the Northeastern states exhibited wind speeds at 100 m a.g.l. that exceeded the locally determined U_{999} (Fig. 3). The 8^{th} most intense windstorm (Table 2) is the “Storm of the Century” of 12-14 March 1993 that formed in the Gulf of Mexico and caused widespread damage in Florida and along the Atlantic coast before entering the Northeast (Huo et al., 1995).

The synoptic-scale structure of extra-tropical cyclones is complicated (Hoskins, 1990). Generally, but not uniformly, maximum wind speeds are associated with low-level jets that occur along the cold fronts of extra-tropical cyclones (Hoskins, 1990;Browning, 2004). Consistent with that expectation, the centroid of ERA5 grid cells with $U>U_{999}$ tends to move in parallel with the cyclone track locations but are generally displaced to the south/southeast (Fig. 2).

https://doi.org/10.5194/nhess-2020-345
Preprint. Discussion started: 11 December 2020

Natural Hazards and Earth System Sciences
Discussions

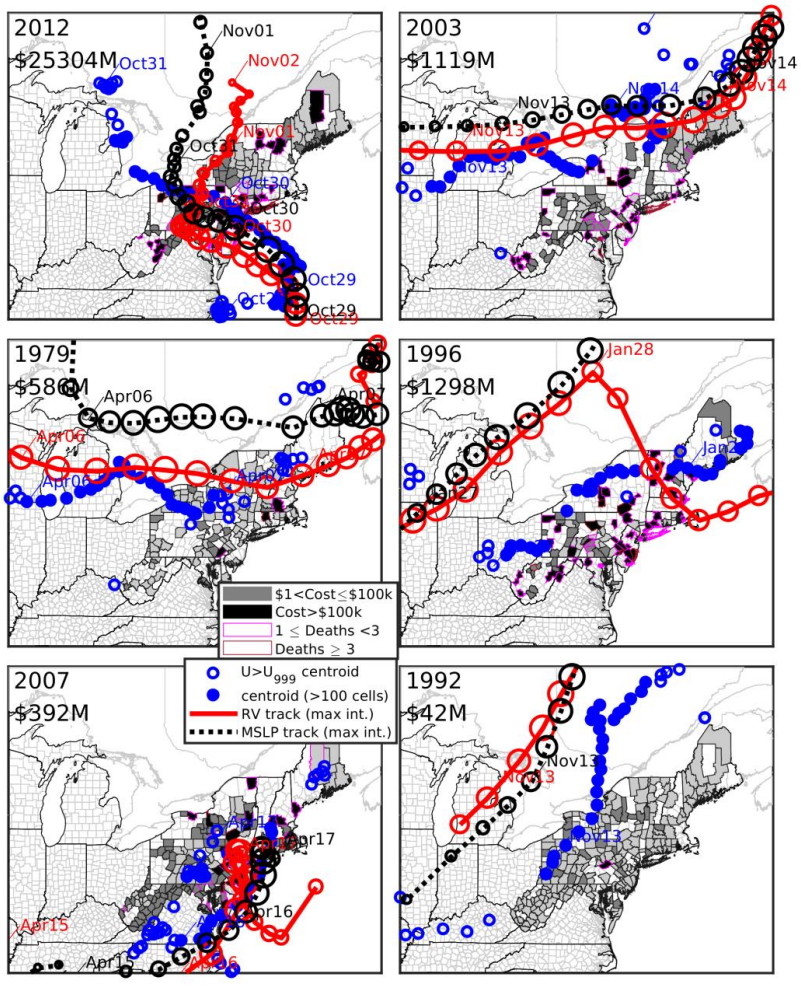

340 **Figure 2. Windstorm centers as the geographic center of all ERA5 grid cells for U > U_{999} (blue). Markers are filled when there are >100 cells over this threshold. Timing and location of the cyclone centers as diagnosed from MSLP and relative vorticity at 700 hPa are shown in black and red, respectively. Markers every 3 hours along each track have a diameter corresponding to track intensity. The underlying shading shows the county-level damage and deaths in the Northeastern states associated with each event as diagnosed from the NOAA storm reports.**

https://doi.org/10.5194/nhess-2020-345
Preprint. Discussion started: 11 December 2020

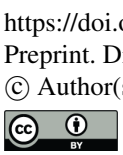

Natural Hazards and Earth System Sciences
Discussions

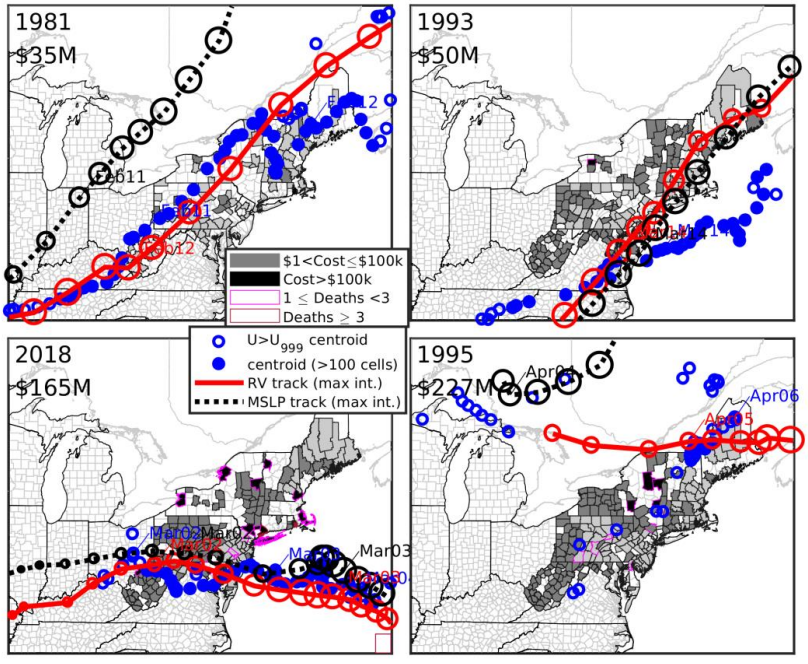

Figure 2 (cont).

Previous research has reported that reinsurance contracts commonly employ a 72 hour window to describe a 'single event' (Haylock, 2011). All of the windstorms identified in this work transited the Northeastern study domain in < 72 hours. Intense wind coverage ($U>U_{999}$) is generally concentrated in the ±10 hours around the storm peak time, t_p (Fig. 3), although some windstorms had longer duration and a slower decay in widespread intense wind speeds with significant coverage remaining >10 hours after t_p (Fig. 3).

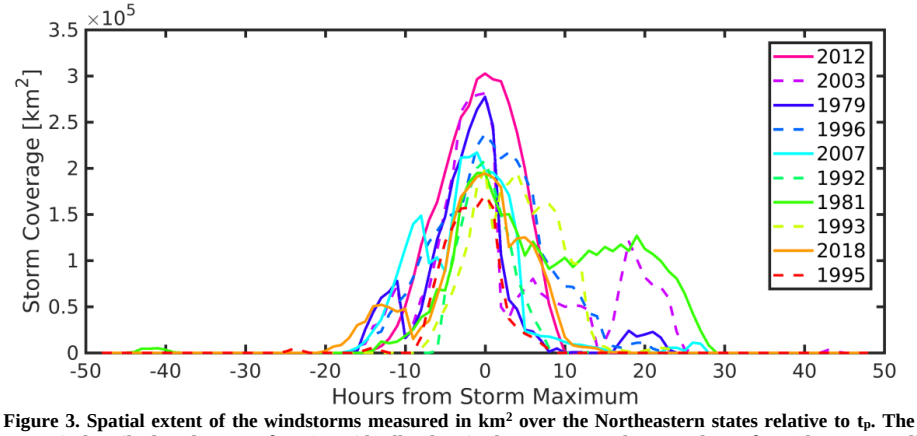

Figure 3. Spatial extent of the windstorms measured in km^2 over the Northeastern states relative to t_p. The spatial extent is described as the area of ERA5 grid cells wherein the $U > U_{999}$. Values are shown for 48 hours preceding and following each windstorm peak.

Twenty-four-hour precipitation totals, used as an indicator of flooding potential, and maximum precipitation rates, used as an indicator of transportation hazards, vary substantially among the ten windstorms, but virtually all of the windstorms were associated with some form of extreme or hazardous precipitation (Fig. 4). Consistent with

https://doi.org/10.5194/nhess-2020-345
Preprint. Discussion started: 11 December 2020

Natural Hazards and Earth System Sciences
Discussions

observational evidence (Munsell and Zhang, 2014), Hurricane Sandy (windstorm during 2012) is associated with total 24-hour precipitation accumulation in several ERA5 grid cells of up to 100 mm, and accumulations exceeded 20 mm in multiple ERA5 grid cells. Very heavy precipitation, both in terms of maximum precipitation intensity and total accumulated precipitation is also associated with the 1993 windstorm resulting from a decaying TC that formed a NE (Fig. 4). The windstorms with lowest precipitation totals occurred in 2003, 1979 and 1995 and are associated with AC. Freezing rain, which in conjunction with high winds is a particular hazard to electrical infrastructure and transportation, is present during the windstorms in 1992, 1981 and 1993 (Fig. 4). There is also snow indicated in at least one location in the domain in every storm, except for 2012 (Hurricane Sandy).

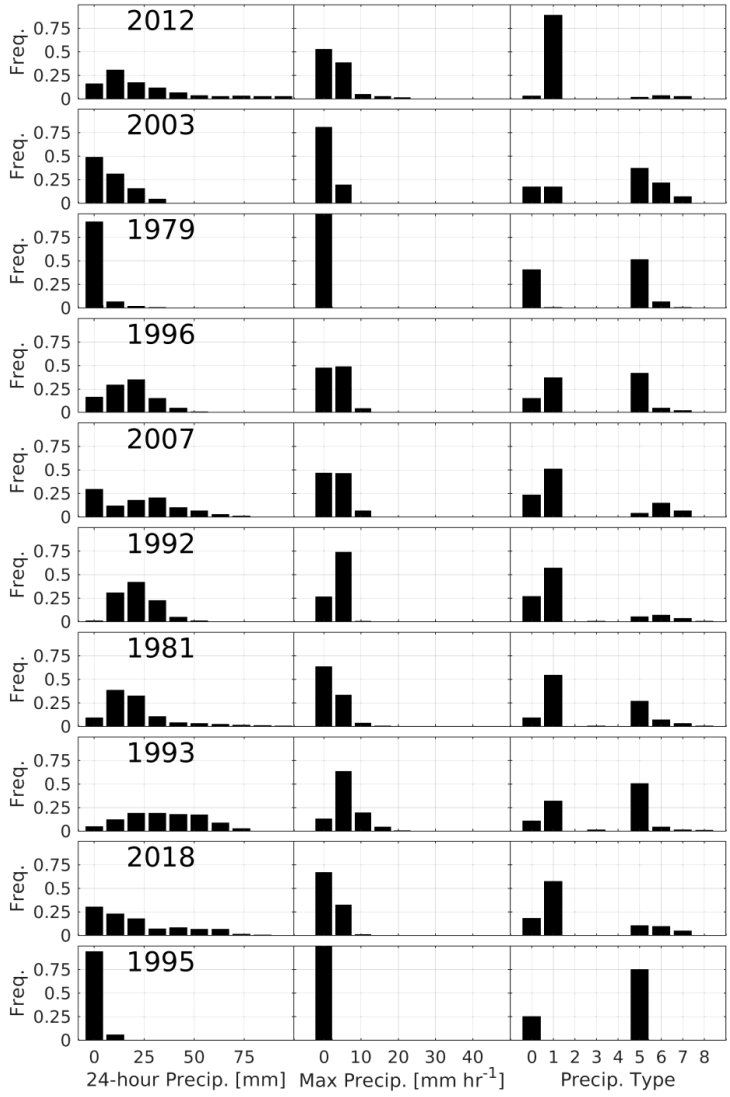

Figure 4. Histograms of precipitation totals and maximum precipitation rates and precipitation types for the 24 hours centered on each storm peak across ERA5 land-based grid cells in the Northeastern states. The frequencies are the fraction of grid cells in each class (out of 924). Precipitation types are as follows: No precipitation (0), rain (1), freezing rain (3), snow (5), wet snow (6), mixture of rain and snow (7) and ice pellets (8).

https://doi.org/10.5194/nhess-2020-345
Preprint. Discussion started: 11 December 2020

Natural Hazards and Earth System Sciences
Discussions

375 Four of the top-10 windstorms occurred after 2000 (2012, 2003, 2007 and 2018, Table 2), and thus high quality ASOS and RADAR data are available for comparison with estimates from ERA5 for these events. For the 2012, 2003 and 2018 windstorms there is good agreement between the spatial extent of locally extreme wind speeds from ERA5 and ASOS, and the duration of intense wind speeds (Fig. 5). The agreement is less good for the 2007 windstorm possibly due to the low density of ASOS stations in the U.S. state of Maine where the ERA5 output
380 indicate the wind maximum was manifest for a substantial fraction of the storm period (Fig. 2). For the other three windstorms the fraction of ERA5 grid cells in the Northeastern states with $U>U_{999}$ closely matches the fraction of ASOS stations in the same area that exceed their local U_{999} threshold during each hour of the storm period (Fig. 5). The timing of storm precipitation in the ERA5 data is also in good agreement with observational estimates from RADAR and ASOS stations, consistent with assimilation of RADAR precipitation and weather station data
385 (Lopez, 2011;Hersbach et al., 2019). The period with most intense precipitation occurred concurrently with the high wind speeds during Hurricane Sandy, but largely well before t_p in the 2007 and 2018 windstorms (Fig. 5), consistent with previous work characterizing extra-tropical cyclones (Bengtsson et al., 2009). Mean ERA5 precipitation rates in Northeast states during these ten storms are consistently somewhat higher than estimates from RADAR, but below ASOS point measurements, reflecting spatial variability in rainfall intensity at scales
390 below those manifest in a network of point measurements (Villarini et al., 2008).

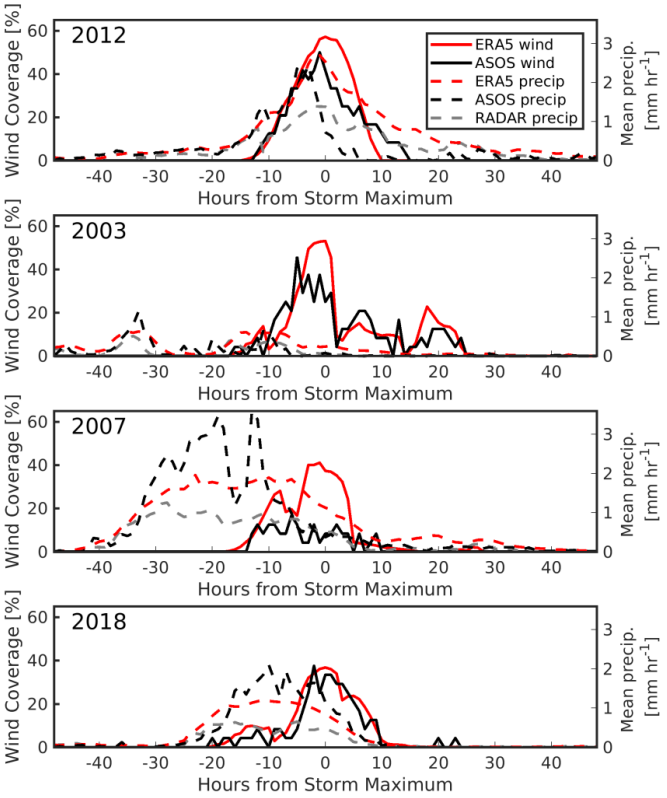

Figure 5. Time series of high wind coverage and mean precipitation rate during the four windstorms that occurred after the year 2000. Each subplot includes the fraction of ERA5 grid cells with over-threshold wind speeds ($U > U_{999}$), the number of ASOS stations with over-threshold wind speeds, the mean precipitation rate (in land areas of Northeast
395 **states within 200 km of a RADAR station) from ERA5, NWS RADAR and ASOS point observations.**

https://doi.org/10.5194/nhess-2020-345
Preprint. Discussion started: 11 December 2020


Natural Hazards and Earth System Sciences
Discussions

A larger sample of 50 windstorms was also drawn from the 40-year time series to examine the serial dependence. These top-50 windstorms are relatively well described by a Poisson distribution in terms of counts per calendar year. The resulting dispersion value (D) is 0.18 indicating evidence for serial dependence or alternatively stated that these windstorms are clustered in fewer years than would be expected for independent events. Of 10,000 bootstrapped samples, 99.97% had dispersion indices above zero. While this D value is symptomatic of serial clustering for windstorms that impact the Northern USA, it is lower than those computed for regions of European in earlier research using the 20th century ERA reanalysis and a 98th percentile wind speed threshold (Walz et al., 2018). While the top ten windstorms considered in detail herein all have spatial extent of between 309 and 524 grid cells, the 11th- through 50th-ranked storms in the set used to characterize seriality have a mean extent of 216 grid cells, and range in extent from 176 to 309 cells, further indicating that the top ten storms are distinct in the 40-year time series (Fig. 1).

3.2 Cyclone detection and tracking

Consistent with past research employing other reanalysis data sets (Ulbrich et al., 2009), results from application of the cyclone detection and tracking algorithm to ERA5 output also indicate the U.S. Northeast exhibits a high frequency of transitory cyclones (Fig. 6). Also in accord with expectations, the tracks followed by the windstorms are generally characteristic of those dominant cyclone tracks, and derive from a mixture of intense nor'easters (NE), Alberta Clippers (AC), deep Colorado lows (CL), and decaying tropical cyclones (TC) (Table 3, Fig. 6). Cyclone intensities for the 10 windstorms are an order of magnitude above the mean intensities for cold-weather cyclones at the same locations over the U.S. for both RV and MSLP (Fig. 7, Table 3). Windstorms with the highest intensities tend to pass over the ocean (2012, 1993 and the 2018 storm). Both the 2012 and the 1993 windstorms are the result of decaying tropical cyclones, with the 1993 system transitioning to become a NE (Fig. 2 and 6, Table 3). The 2012 windstorm (Hurricane Sandy) exhibited extremely high intensity and is also associated with the largest area (number of grid cells) with $U>U_{999}$. It was also associated with by far the largest amount of property damage and deaths (Fig. 2, Table 2). The 2018 windstorm is associated with a CL that stalled over the Atlantic coast and re-intensified to form a NE. Although this event was not the most geographically expansive, its track over very high-density population areas and high value assets led to high associated storm damage (Fig. 2). Five of the 10 storms are associated with Colorado Lows, consistent with the high prevalence of such cyclones (Booth et al., 2015) (Fig. 6). These storms generally impacted the smallest areas and tend to be associated with substantial but lower amounts of property damage than TC or AC (Table 2).

The Great Lakes are known to have a profound effect on passing cyclones during ice-free and generally unstable conditions that prevail during September to November (Angel and Isard, 1997). Particularly during the early part of the cold-season, cyclones that cross the Great Lakes are frequently subject to acceleration and intensification via enhanced vertical heat flux and low-level moisture convergence due to the lake-land roughness contrast (Xiao et al. 2018). Cyclones that transit the Great Lakes during periods with substantial ice cover are subject to less alteration (Angel and Isard, 1997). The 2003, 1979 and 1995 storms are associated with Alberta Clippers (Table 3) that exhibit initially low intensities, but rapidly intensify as they pass across the Great Lakes region (~80°W and 45°N). Cyclone intensities for these three storms increased by an average of 16% for RV and 33% for MSLP during their crossing of the Great-Lakes longitudes (92°W to 76°W). These windstorms occurred when Great Lakes ice cover was minimal (https://www.glerl.noaa.gov/data/ice/atlas/ice_duration/duration.html). Both 2003

https://doi.org/10.5194/nhess-2020-345
Preprint. Discussion started: 11 December 2020

Natural Hazards and Earth System Sciences
Discussions

and 1979 storms events exhibit large spatial scales (Fig. 3) and resulted in substantial property damage (Table 2). Tracking of windstorms is a key determinant of societal impacts. The 2012 and 2017 windstorms had high-wind speed centroids that are closely aligned from the cyclone centers. They passed over highly populated areas including New York, and are associated with recorded damage in the hundreds of millions of dollars (Fig. 2, Table 2). The 1993 windstorm high wind speed centroid is out over the Atlantic Ocean which may partly explain the lower loss of life and property damage associated with this event (Fig. 2). The AC associated windstorms (2003, 1979, 1995) tracked west-east have maximum intensity centers across the north of the region and thus were also associated with lower damages over the US than other the other windstorms. Cyclones associated with the windstorms in 1992, 1996, 1981 tracked from the southeast to the northwest but their centers diagnosed from MSLP remain east of the region as do those from RV in 1992 and 1996. The geographic centroids of high wind speeds track through Virginia, Pennsylvania, and New York in all three years. Inflation-adjusted damage amounts are very different for these storms and range from $24 million for the 1981 windstorm to $2181 million for the 1996 windstorm (Fig. 2 and 7).

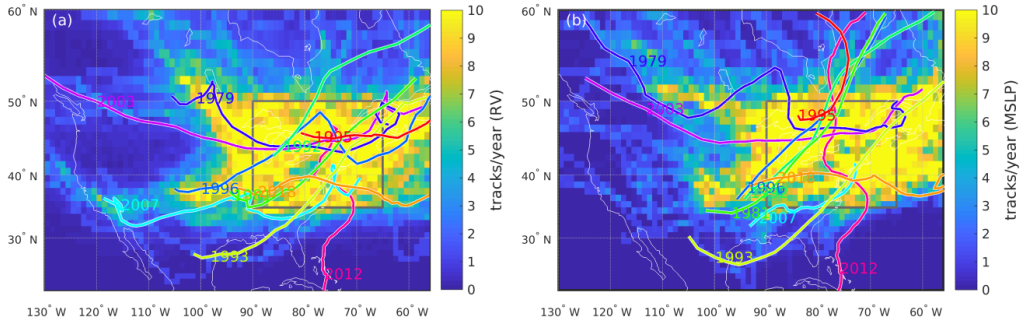

Figure 6. Cyclone tracks associated with each of the top 10 windstorms (individual colors) plotted over a heat map of cyclone densities. Cyclone frequencies are computed at the ERA5 grid resolution and then averaged to a 1°×1° grid to aid legibility. These densities include only cyclones that track within the Northeast rectangle (shown in grey) during cold months (October-April 1979-2018) for (a) relative vorticity and (b) MSLP. Color coding of the cyclone tracks associated with each windstorm is as in Fig. 3.

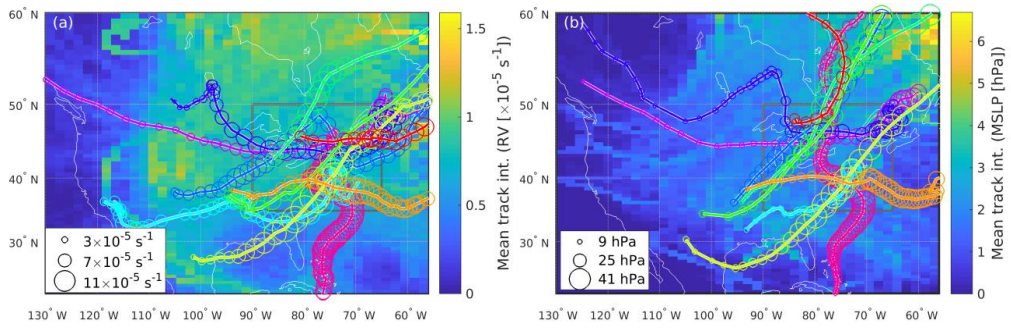

Figure 7. Cyclone intensities for analyses of (a) 700 hPa relative vorticity and (b) mean sea level pressure (shown as an absolute value) for each of the top 10 windstorms (where the symbol diameter scales with intensity) plotted over a heat map of mean cyclone intensities. Cyclone intensities are computed at the ERA5 grid resolution and then averaged to a 1°×1° grid to aid legibility. These intensities include only cyclones that track within the Northeast rectangle (shown in grey) during cold months (October-April 1979-2018) and are anomalies identified in the filtered fields, obtained from the spectral filtering which has the large scale background removed for the tracking. Symbol sizes shown in the figure legends represent the 10th, 50th and 90th percentile cyclone intensities from among the top 10 windstorms, and color coding of the cyclone tracks associated with each windstorm is as in Fig. 3 and Fig. 6.

https://doi.org/10.5194/nhess-2020-345
Preprint. Discussion started: 11 December 2020

Natural Hazards and Earth System Sciences
Discussions

3.3 Windstorm Return Periods

All ten windstorms are associated with long return-period (RP > 50 years) wind speeds in at least some ERA5 grid cells, with return periods exceeding 100 years for the 2012 windstorm. Defining a single return period for each windstorm is difficult due to the multiple degrees of freedoms, but the median (50th percentile) and highest 5 percent (95th percentile) of ERA5 grid cell estimates provide some qualitative assessment of probability. The median RP computed for all 924 grid cells ranges from 1 to 5 years across the ten windstorms (Table 3), while at least 5% of grid cells are characterized by wind speeds during each of the ten windstorms with RP of 6.5 to 106 years (Table 3, Fig. 8). The number of ERA5 grid cells that exhibit the annual maximum during the storm period are positively correlated with the three metrics of return periods; (i) median RP, (ii) 95th percentile RP and (iii) median RP for grid cells that exhibited $U>U_{999}$ (r: 0.45 to 0.64), consistent with the longest-RP wind speeds being associated with the largest windstorms (Fig. 8, Table 3). For the two windstorms that entered the Northeastern states from the Atlantic (2012 and 1993), high-RP wind speeds are concentrated along the coast. The 2003 and 1979 windstorms, the highest-magnitude Alberta Clippers, are associated with extreme high return-period wind speeds in the Great Lakes region. Wind speeds over a large number of grid cells over and around the Great Lakes exhibited their 50-year RP estimates during the 1979 windstorm. Indeed, this windstorm, while not the most spatially expansive (Table 2), is the event with the largest number of ERA5 grid cells in excess of 50-year RP wind speeds in the Northeast domain. The Colorado Low associated windstorms (1996, 2007 and 1981) have their highest-RP winds in the mountainous regions of West Virginia, New York, Vermont, and Maine (WV, NY, VT, and ME).

Table 3. Windstorm details (windstorms are ordered as in Table 2). Cyclone type is based on subjective evaluation of results from the cyclone detection and tracking algorithm: AC = Alberta Clipper. TC = Tropical Cyclone. CL = Colorado Low. NE = Nor'easter. Max intensity is the maximum cyclone intensity along the storm-associated cyclone tracks for RV (x10^{-5} s^{-1}) and MSLP (scaled by -1, hPa). # cells with U_{max} indicates the number of grid cells for which the maximum wind speed for the storm year occurred within the storm period. Median RP is the 50th percentile return period for maximum wind speed in each Northeastern grid cells during each storm period, while p95 is the 95th percentile RP. Also shown is the median RP for grid cells that exhibited $U>U_{999}$ at the storm peak.

Cyclone type	Cyclone track start			Cyclone track end			Max intensity: RV [10^{-5} s^{-1}] / MSLP [-1 hPa]	# cells with U_{max}	Median RP [years]	p_{95} RP [years]	Median RP of cells exceeding U_{999} [years]
	Time	Lat [°N]	Lon [°W]	Time	Lat [°N]	Lon [°W]					
TC	10/18/2012 09:00	11.61	61.10	11/2/2012 00:00	46.92	74.95	14.3/49.1	530	4.56	105.78	12.22
AC	11/11/2003 00:00	52.97	129.82	11/23/2003 06:00	50.39	68.5	10.5/36.9	494	2.30	34.88	5.47
AC	4/4/1979 00:00	50.61	105.62	4/8/1979 21:00	46.98	63.88	10.0/32.1	412	1.55	43.57	6.38
CL	1/26/1996 00:00	37.91	105.01	2/1/1996 06:00	57.08	41.55	10.5/45.4	488	3.54	19.35	5.08
CL/NE	4/11/2007 21:00	36.44	118.73	4/17/2007 18:00	39.56	69.32	12.4/39.6	462	1.58	18.14	3.73
CL	11/12/1992 21:00	42.71	86.00	11/15/1992 12:00	57.06	45.63	11.2/50.1	343	1.45	6.51	3.01
CL	2/11/1981 00:00	37.44	94.50	2/16/1981 06:00	63.41	37.65	8.9/56.3	523	2.23	22.19	6.57
TC/NE	3/12/1993 06:00	27.37	101.40	3/15/1993 18:00	51.88	52.39	15.3/49.2	536	2.12	36.77	5.42
CL	3/1/2018 03:00	38.14	93.72	3/6/2018 06:00	42.13	53.31	13.3/40.9	310	1.03	14.05	4.92
AC	4/4/1995 15:00	45.88	80.74	4/10/1995 06:00	62.63	58.16	9.5/24.2	94	1.00	14.38	2.30

https://doi.org/10.5194/nhess-2020-345
Preprint. Discussion started: 11 December 2020

Natural Hazards and Earth System Sciences
Discussions
Open Access
EGU

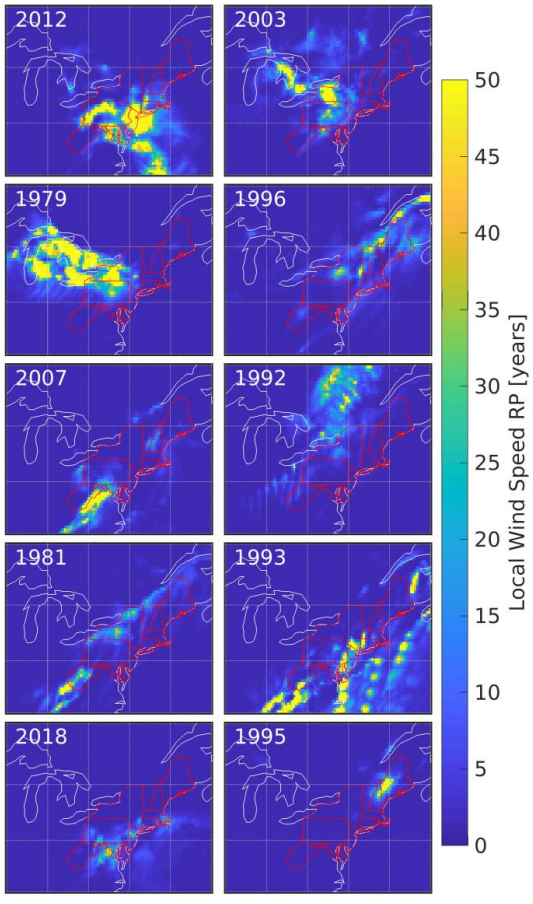

Figure 8. Return period (in years) of storm-maximum wind speed (U_{peak}) in each ERA5 grid cell associated with each windstorm. The color scale is truncated at 50 years but, for example, the maximum return period value during Hurricane Sandy exceeds 100 years for multiple grid cells. Northeastern state borders are shown in red and coastlines (Atlantic Ocean and Great Lakes) are shown in white.

4 Concluding Remarks

The U.S. Northeast exhibits high socio-economic exposure to atmospheric hazards due to the presence of major urban centers with high population density and high density of insured, high-value assets (Table 1, Fig. 1), and windstorms present a substantial fraction of historically important climate hazards in this region. The Northeastern states are also experiencing population increases that are projected to continue into the future (Zoraghein and O'Neill, 2020). This increase in population may result in increased exposure to this hazard even in the absence of any change in windstorm frequency or intensity. Thus, there is great value in improved characterization of these events.

The ten largest windstorms in the Northeast U.S. during 1979-2018 covered 33 to 57% of ERA5 land cells in the Northeastern states with wind speeds exceeding the locally determined 99.9th percentile threshold (Table 2). Although all ten events occurred during the cool season months of October through April, they are distributed throughout the forty-years, and no individual year exhibits more than one of these events (Fig. 1b). However,

https://doi.org/10.5194/nhess-2020-345
Preprint. Discussion started: 11 December 2020


Natural Hazards and Earth System Sciences
Discussions

when a larger pool of the top 50 largest windstorms is considered, clear evidence of serial clustering emerges. Return periods for wind speeds in the upper 5% of ERA5 grid cells during these 10 windstorms range from 6.5 to 106 years (Table 3, Fig. 8). Many of these windstorms exhibit co-occurrence of extreme and/or hazardous precipitation and thus may be considered composite events.

Any windstorm catalogue is, to some degree, a product of the dataset on which it is predicated, and the windstorms identified herein are derived using a methodology that preferences intense but large-scale events. Their characteristics will naturally differ from severe local storms. The windstorms identified independently and objectively in this work are consistent with historically notable events. Further, precipitation and wind speeds from ERA5 for windstorms that occurred after 2000 exhibit good agreement with in-situ observations from the NWS ASOS network and NWS dual-polarization RADAR, consistent with assimilation RADAR precipitation and weather station data streams by the ECMWF data assimilation protocols and past evaluations of the ERA5 reanalysis (Fig. 5). The accord between the geophysical data streams and the ERA5 windstorm intensity estimates and independent damage estimates provide further confidence in the fidelity of the windstorm catalogue presented herein.

The cyclone tracks associated with the ten windstorms are consistent with the climatology of cold-season cyclones and thus the associated extra-tropical cyclones are a mixture of; Alberta Clippers, Colorado Lows, decaying Tropical Cyclones and Nor' easters (Fig. 6). These cyclones, however, exhibit considerably higher intensities (from both RV and MSLP perturbations) that are an order of magnitude higher than mean values sampled on those same tracks (Fig. 7). With the possible exception of Hurricane Sandy, these windstorms are largely differentiable from the cyclone climatology in terms of their intensification rather than the associated cyclone storm track. It is also notable that the most intense AC events occurred during periods of low ice cover in the Great Lakes, which may imply windstorms associated with AC events are likely to intensify under climate change as results of reduced icing of these water bodies (Smith, 1991).

Inflation-adjusted (to January 2020) property damage totals for each of the windstorms range from $24 million to $29 billion (Table 2). While there is not perfect agreement in the ranking of these storms between high wind coverage and property damage, the top four storms in terms of extent do all have higher damage totals than the next six.

This windstorm catalogue is intended to characterize extreme windstorms in the Northeastern U.S. and may have value in efforts to evaluate the validate climate and natural hazard catastrophe models. Planned extension of the ERA5 reanalysis to 1950 may provide an opportunity to further extend this analysis to include elements related to non-stationarity in windstorm probability, with the caveat that such detection will be challenging due to changes in the assimilated data. Research is underway to dynamically downscale these windstorms using the Weather Research and Forecasting model to examine sub-grid scale variability in extreme wind speeds and the sensitivity of these events to global climate non-stationarity.

Acknowledgments

This work is support by the U.S. Department of Energy (DoE) (DE-SC0016438 and DE-SC0016605), and used computing resources from the National Science Foundation: Extreme Science and Engineering Discovery Environment (XSEDE) (allocation award to SCP is TG-ATM170024).

https://doi.org/10.5194/nhess-2020-345
Preprint. Discussion started: 11 December 2020

Natural Hazards and Earth System Sciences
Discussions

Data Availability

ERA5 reanalysis output are available from https://climate.copernicus.eu/climate-reanalysis. NWS RADAR data are available from the National Climatic Data Center; https://www.ncdc.noaa.gov/data-access/radar-data. NWS ASOS data are available from ftp://ftp.ncdc.noaa.gov/pub/data/asos-fivemin/. The NOAA Storms database is available at; https://www.ncdc.noaa.gov/stormevents/. Historical estimates of Great Lakes ice cover are available from: https://www.glerl.noaa.gov/data/ice/atlas/ice_duration/duration.html.

Author Contribution

All four authors participated discussion about the goals and methods for this paper. SCP devised the analysis framework. FL had primary responsibility for performing the analyses. FL, SCP and RJB wrote the majority of the manuscript text. KH provided analysis tools, expertise, advice and context for cyclone tracking. RJB and SCP performed analyses on the societal impact of these windstorms. RJB and SCP acquired the funding and computing resources to make this research possible.

Competing Interests

The authors declare that they have no conflict of interest.

References

Baldini, L. M., Baldini, J. U., McElwaine, J. N., Frappier, A. B., Asmerom, Y., Liu, K.-b., Prufer, K. M., Ridley, H. E., Polyak, V., and Kennett, D. J.: Persistent northward North Atlantic tropical cyclone track migration over the past five centuries, Scientific reports, 6, 37522, 2016.

Bao, M., Ding, Y., Sang, M., Li, D., Shao, C., and Yan, J.: Modeling and evaluating nodal resilience of multi-energy systems under windstorms, Applied Energy, 270, 115136, 2020.

Befort, D. J., Wild, S., Kruschke, T., Ulbrich, U., and Leckebusch, G. C.: Different long-term trends of extra-tropical cyclones and windstorms in ERA-20C and NOAA-20CR reanalyses, Atmospheric Science Letters, 17, 586-595, 2016.

Bengtsson, L., Hagemann, S., and Hodges, K. I.: Can climate trends be calculated from reanalysis data?, Journal of Geophysical Research: Atmospheres, 109, 2004.

Bengtsson, L., Hodges, K. I., and Keenlyside, N.: Will extratropical storms intensify in a warmer climate?, Journal of Climate, 22, 2276-2301, 2009.

Bentley, A. M., Bosart, L. F., and Keyser, D.: A climatology of extratropical cyclones leading to extreme weather events over central and eastern North America, Monthly Weather Review, 147, 1471-1490, 2019.

Bierly, G. D., and Harrington, J. A.: A Climatology of Transition Season Colorado Cyclones - 1961-1990, Journal of Climate, 8, 853-863, 1995.

Bloomfield, H., Shaffrey, L., Hodges, K., and Vidale, P.: A critical assessment of the long-term changes in the wintertime surface Arctic Oscillation and Northern Hemisphere storminess in the ERA20C reanalysis, Environmental Research Letters, 13, 094004, 2018.

Booth, J. F., Rieder, H. E., Lee, D. E., and Kushnir, Y.: The paths of extratropical cyclones associated with wintertime high-wind events in the northeastern United States, Journal of Applied Meteorology and Climatology, 54, 1871-1885, 2015.

Bouwer, L. M., Crompton, R. P., Faust, E., Höppe, P., and Pielke Jr, R. A.: Confronting disaster losses, Science, 318, 753, 2007.

Brönnimann, S., Martius, O., von Waldow, H., Welker, C., Luterbacher, J., Compo, G. P., Sardeshmukh, P. D., and Usbeck, T.: Extreme winds at northern mid-latitudes since 1871, Meteorologische Zeitschrift, 21, 13-27, 2012.

Brown, T. M., Pogorzelski, W. H., and Giammanco, I. M.: Evaluating hail damage using property insurance claims data, Weather, Climate, and Society, 7, 197-210, 2015.

https://doi.org/10.5194/nhess-2020-345
Preprint. Discussion started: 11 December 2020

Natural Hazards and Earth System Sciences
Discussions

Browning, K.: The sting at the end of the tail: Damaging winds associated with extratropical cyclones, Quarterly Journal of the Royal Meteorological Society, 130, 375-399, 2004.

Census, U. S.: State Population Totals and Components of Change: 2010-2019: https://www.census.gov/data/tables/time-series/demo/popest/2010s-state-total.html, access: September 10, 2020, 2019.

Changnon, S. A.: Temporal and spatial distributions of wind storm damages in the United States, Climatic Change, 94, 473-482, 2009.

Clark, P. A., and Gray, S. L.: Sting jets in extratropical cyclones: a review, Quarterly Journal of the Royal Meteorological Society, 144, 943-969, 2018.

Cunha, L. K., Smith, J. A., Krajewski, W. F., Baeck, M. L., and Seo, B.-C.: NEXRAD NWS polarimetric precipitation product evaluation for IFloodS, Journal of Hydrometeorology, 16, 1676-1699, 2015.

Della-Marta, P. M., Mathis, H., Frei, C., Liniger, M. A., Kleinn, J., and Appenzeller, C.: The return period of wind storms over Europe, International Journal of Climatology, 29, 437-459, 10.1002/joc.1794, 2009.

Dörenkämper, M., Olsen, B. T., Witha, B., Hahmann, A. N., Davis, N. N., Barcons, J., Ezber, Y., García-Bustamante, E., González-Rouco, J. F., and Navarro, J.: The Making of the New European Wind Atlas–Part 2: Production and Evaluation, Geoscientific Model Development, 13, 5079-5102, 2020.

Feser, F., Barcikowska, M., Krueger, O., Schenk, F., Weisse, R., and Xia, L.: Storminess over the North Atlantic and northwestern Europe—A review, Quarterly Journal of the Royal Meteorological Society, 141, 350-382, 2015.

Gall, M., Borden, K. A., and Cutter, S. L.: When do losses count? Six fallacies of natural hazards loss data, Bulletin of the American Meteorological Society, 90, 799-810, 2009.

Gall, M., Borden, K. A., Emrich, C. T., and Cutter, S. L.: The unsustainable trend of natural hazard losses in the United States, Sustainability, 3, 2157-2181, 2011.

Golden, J. H., and Snow, J. T.: Mitigation against extreme windstorms, Reviews of Geophysics, 29, 477-504, 1991.

Gramcianinov, C., Campos, R., de Camargo, R., Hodges, K., Soares, C. G., and da Silva Dias, P.: Analysis of Atlantic extratropical storm tracks characteristics in 41 years of ERA5 and CFSR/CFSv2 databases, Ocean Engineering, 216, 108111, 2020.

Halverson, J. B., and Rabenhorst, T.: Hurricane Sandy: The science and impacts of a superstorm, Weatherwise, 66, 14-23, 2013.

Haylock, M. R.: European extra-tropical storm damage risk from a multi-model ensemble of dynamically-downscaled global climate models, Natural Hazards and Earth System Sciences, 11, 2847, 2011.

Hersbach, H., Bell, B., Berrisford, P., Horányi, A., Sabater, J. M., Nicolas, J., Radu, R., Schepers, D., Simmons, A., and Soci, C.: Global reanalysis: goodbye ERA-Interim, hello ERA5, ECMWF Newsl, 159, 17-24, 2019.

Hersbach, H., Bell, B., Berrisford, P., Hirahara, S., Horányi, A., Muñoz-Sabater, J., Nicolas, J., Peubey, C., Radu, R., and Schepers, D.: The ERA5 global reanalysis, Quarterly Journal of the Royal Meteorological Society, 146, 1999-2049, 2020.

Hewson, T. D., and Neu, U.: Cyclones, windstorms and the IMILAST project, Tellus A: Dynamic Meteorology and Oceanography, 67, 27128, 2015.

Hirsch, M. E., DeGaetano, A. T., and Colucci, S. J.: An East Coast winter storm climatology, Journal of Climate, 14, 882-899, 2001.

Hobbs, P. V., Locatelli, J. D., and Martin, J. E.: A new conceptual model for cyclones generated in the lee of the Rocky Mountains, Bulletin of the American Meteorological Society, 77, 1169-1178, 1996.

Hodges, K. I., Lee, R. W., and Bengtsson, L.: A Comparison of Extratropical Cyclones in Recent Reanalyses ERA-Interim, NASA MERRA, NCEP CFSR, and JRA-25, Journal of Climate, 24, 4888-4906, 10.1175/2011jcli4097.1, 2011.

Hoskins, B. J.: Theory of extratropical cyclones, in: Extratropical Cyclones, edited by: Newton, C. W., and Holopainen, E. O., American Meteorological Society, Boston, MA, American Meteorological Society, Boston, MA. ISBN: 978-1-944970-33-8, 63-80, 1990.

Hoskins, B. J., and Hodges, K. I.: New perspectives on the Northern Hemisphere winter storm tracks, Journal of the Atmospheric Sciences, 59, 1041-1061, 2002.

Huo, Z., Zhang, D.-L., Gyakum, J., and Staniforth, A.: A diagnostic analysis of the superstorm of March 1993, Monthly Weather Review, 123, 1740-1761, 1995.

Jeong, D. I., Cannon, A. J., and Zhang, X.: Projected changes to extreme freezing precipitation and design ice loads over North America based on a large ensemble of Canadian regional climate model simulations, Natural Hazards & Earth System Sciences, 19, 857-872, 2019.

Jourdier, B.: Evaluation of ERA5, MERRA-2, COSMO-REA6, NEWA and AROME to simulate wind power production over France, Advances in Science and Research, 17, 63-77, 2020.

Kalverla, P. C., Duncan Jr, J. B., Steeneveld, G. J., and Holtslag, A. A. M.: Low-level jets over the North Sea based on ERA5 and observations: together they do better, Wind Energy Science, 4, 193-209, https://10.5194/wes-4-193-2019, 2019.

https://doi.org/10.5194/nhess-2020-345
Preprint. Discussion started: 11 December 2020

Natural Hazards and Earth System Sciences
Discussions

Kalverla, P. C., Holtslag, A. A. M., Ronda, R. J., and Steeneveld, G. J.: Quality of wind characteristics in recent wind atlases over the North Sea, Quarterly Journal of the Royal Meteorological Society, Available in early view, DOI: 10.1002/qj.3748, 10.1002/qj.3748, 2020.

Kitzmiller, D., Miller, D., Fulton, R., and Ding, F.: Radar and multisensor precipitation estimation techniques in National Weather Service hydrologic operations, Journal of Hydrologic Engineering, 18, 133-142, 2013.

Klawa, M., and Ulbrich, U.: A model for the estimation of storm losses and the identification of severe winter storms in Germany, Natural Hazards and Earth System Sciences, 3 (6), 725-732, 2003.

Konisky, D. M., Hughes, L., and Kaylor, C. H.: Extreme weather events and climate change concern, Climatic Change, 134, 533-547, 10.1007/s10584-015-1555-3, 2016.

Krajewski, W., and Smith, J. A.: Radar hydrology: rainfall estimation, Advances in water resources, 25, 1387-1394, 2002.

Kreibich, H., Van Den Bergh, J. C., Bouwer, L. M., Bubeck, P., Ciavola, P., Green, C., Hallegatte, S., Logar, I., Meyer, V., and Schwarze, R.: Costing natural hazards, Nature Climate Change, 4, 303-306, 2014.

Lackmann, G. M.: Hurricane Sandy before 1900 and after 2100, Bulletin of the American Meteorological Society, 96, 547-560, 2015.

Lamb, H.: Historic Storms of the North Sea, British Isles and Northwest Europe, Cambridge University Press. ISBN: 978-0521619318, 228 pp., 1991. 0521375223

Lareau, N. P., and Horel, J. D.: The climatology of synoptic-scale ascent over western North America: A perspective on storm tracks, Monthly Weather Review, 140, 1761-1778, 2012.

Larsén, X. G., Ott, S., Badger, J., Hahmann, A. N., and Mann, J.: Recipes for correcting the impact of effective mesoscale resolution on the estimation of extreme winds, Journal of Applied Meteorology and Climatology, 51, 521-533, 2012.

Letson, F., Barthelmie, R. J., and Pryor, S. C.: RADAR-derived precipitation climatology for wind turbine blade leading edge erosion, Wind Energy Science, 5, 331-347, 2020.

Li, F., Chavas, D. R., Reed, K. A., and Dawson II, D. T.: Climatology of severe local storm environments and synoptic-scale features over North America in ERA5 reanalysis and CAM6 simulation, Journal of Climate, 33, 8339-8365, 2020.

Lopez, P.: Direct 4D-Var assimilation of NCEP stage IV radar and gauge precipitation data at ECMWF, Monthly Weather Review, 139, 2098-2116, 2011.

Lukens, K. E., Berbery, E. H., and Hodges, K. I.: The imprint of strong-storm tracks on winter weather in North America, Journal of Climate, 31, 2057-2074, 2018.

Ma, C.-G., and Chang, E. K.: Impacts of Storm-Track Variations on Wintertime Extreme Weather Events over the Continental United States, Journal of Climate, 30, 4601-4624, 2017.

Mailier, P. J., Stephenson, D. B., Ferro, C. A., and Hodges, K. I.: Serial clustering of extratropical cyclones, Monthly weather review, 134, 2224-2240, 2006.

Mann, J., Kristensen, L., and Jensen, N. O.: Uncertainties of extreme winds, spectra, and coherences, in: Bridge Aerodynamics, edited by: Larsen, and Esdahl, Balkerna, Rotterdam, 49-56, 1998.

Marchigiani, R., Gordy, S., Cipolla, J., Adams, R. C., Evans, D. C., Stehly, C., Galwankar, S., Russell, S., Marco, A. P., and Kman, N.: Wind disasters: A comprehensive review of current management strategies, International journal of critical illness and injury science, 3, 130, 2013.

Mills, E., and Jones, R. B.: An insurance perspective on US electric grid disruption costs, The Geneva Papers on Risk and Insurance-Issues and Practice, 41, 555-586, 2016.

Minola, L., Zhang, F., Azorín-Molina, C., Safaei Pirooz, A. A., Flay, R., Hersbach, H., and Chen, D.: Near-surface mean and gust wind speeds in ERA5 across Sweden: towards an improved gust parametrization, Climate Dynamics, 55, 887–907, https://doi.org/10.1007/s00382-020-05302-6, 2020.

Munsell, E. B., and Zhang, F.: Prediction and uncertainty of Hurricane Sandy (2012) explored through a real-time cloud-permitting ensemble analysis and forecast system assimilating airborne Doppler radar observations, Journal of Advances in Modeling Earth Systems, 6, 38-58, 2014.

Nadolski, V.: Automated Surface Observing System (ASOS) user's guide, 1998. http://www.nws.noaa.gov/asos/pdfs/aum-toc.pdf, access: January 5, 2018.

Nelli, N. R., Temimi, M., Fonseca, R. M., Weston, M. J., Thota, M. S., Valappil, V. K., Branch, O., Wulfmeyer, V., Wehbe, Y., and Al Hosary, T.: Impact of roughness length on WRF simulated land-atmosphere interactions over a hyper-arid region, Earth and Space Science, 7, e2020EA001165, https://doi.org/10.1029/2020EA001165, 2020.

Nyce, C., Dumm, R. E., Sirmans, G. S., and Smersh, G.: The capitalization of insurance premiums in house prices, Journal of Risk and Insurance, 82, 891-919, 2015.

Olauson, J.: ERA5: The new champion of wind power modelling?, Renewable energy, 126, 322-331, 2018.

Pinto, J. G., Ulbrich, S., Economou, T., Stephenson, D. B., Karremann, M. K., and Shaffrey, L. C.: Robustness of serial clustering of extratropical cyclones to the choice of tracking method, Tellus A: Dynamic Meteorology and Oceanography, 68, 32204, 2016.

https://doi.org/10.5194/nhess-2020-345
Preprint. Discussion started: 11 December 2020

Pryor, S. C., Barthelmie, R. J., Young, D. T., Takle, E. S., Arritt, R. W., Flory, D., Gutowski, W. J., Nunes, A., and Roads, J.: Wind speed trends over the contiguous United States, Journal of Geophysical Research: Atmospheres, 114, doi: 10.1029/2008JD011416, 2009.

Pryor, S. C., Barthelmie, R. J., Clausen, N., Drews, M., MacKellar, N., and Kjellström, E.: Analyses of possible changes in intense and extreme wind speeds over northern Europe under climate change scenarios, Climate Dynamics, 38, 189-208, 2012.

Pryor, S. C., Shepherd, T. J., Bukovsky, M., and Barthelmie, R. J.: Assessing the stability of wind resource and operating conditions, Journal of Physics: Conference Series, 1452, doi: 10.1088/1742-6596/1452/1081/012084, 2020.

Ramon, J., Lledó, L., Torralba, V., Soret, A., and Doblas-Reyes, F. J.: What global reanalysis best represents near-surface winds?, Quarterly Journal of the Royal Meteorological Society, 145, 3236-3251, 2019.

Roberts, J., Champion, A., Dawkins, L., Hodges, K., Shaffrey, L., Stephenson, D., Stringer, M., Thornton, H., and Youngman, B.: The XWS open access catalogue of extreme European windstorms from 1979 to 2012, Natural Hazards and Earth System Sciences, 14, 2487-2501, 2014.

Sadegh, M., Moftakhari, H., Gupta, H. V., Ragno, E., Mazdiyasni, O., Sanders, B., Matthew, R., and AghaKouchak, A.: Multihazard scenarios for analysis of compound extreme events, Geophysical Research Letters, 45, 5470-5480, 2018.

Sainsbury, E. M., Schiemann, R. K., Hodges, K. I., Shaffrey, L. C., Baker, A. J., and Bhatia, K. T.: How Important are Post-Tropical Cyclones for European Windstorm Risk?, Geophysical Research Letters, e2020GL089853, 2020.

Schmitt IV, C. V.: A quality control algorithm for the ASOS ice free wind sensor, Preprints, 13th Conf. on Integrated Observing and Assimilation Systems for Atmosphere, Oceans, and Land Surface, Phoenix, AZ, Amer. Meteor. Soc. A, 2009,

SEDAC: U.S. Census Grids: https://sedac.ciesin.columbia.edu/data/collection/usgrid, access: September 10, 2020.

Seo, B.-C., Dolan, B., Krajewski, W. F., Rutledge, S. A., and Petersen, W.: Comparison of single-and dual-polarization–based rainfall estimates using NEXRAD data for the NASA Iowa Flood Studies project, Journal of Hydrometeorology, 16, 1658-1675, 2015.

Shepherd, T. G., Boyd, E., Calel, R. A., Chapman, S. C., Dessai, S., Dima-West, I. M., Fowler, H. J., James, R., Maraun, D., and Martius, O.: Storylines: an alternative approach to representing uncertainty in physical aspects of climate change, Climatic change, 151, 555-571, 2018.

Sinh, H. N., Lombardo, F. T., Letchford, C. W., and Rosowsky, D. V.: Characterization of Joint Wind and Ice Hazard in Midwestern United States, Nat. Hazards Rev., 17, 04016004, Unsp 04016004, 10.1061/(asce)nh.1527-6996.0000221, 2016.

Skamarock, W. C.: Evaluating mesoscale NWP models using kinetic energy spectra, Monthly Weather Review, 132, 3019-3032, 2004.

Smith, A. B., and Matthews, J. L.: Quantifying uncertainty and variable sensitivity within the US billion-dollar weather and climate disaster cost estimates, Natural Hazards, 77, 1829-1851, 2015.

Smith, J. B.: The potential impacts of climate change on the Great Lakes, Bulletin of the American Meteorological Society, 72, 21-28, 1991.

Stephenson, D. B.: Definition, diagnosis, and origin of extreme weather and climate events, in: Climate extremes and society, edited by: Diaz, H. F., and Murnane, R. J., Cambridge University Press, 11-23, 2008.

Straka, J. M., Zrnić, D. S., and Ryzhkov, A. V.: Bulk hydrometeor classification and quantification using polarimetric radar data: Synthesis of relations, Journal of Applied Meteorology, 39, 1341-1372, 2000.

Sun, C., and Liang, X.-Z.: Improving US extreme precipitation simulation: sensitivity to physics parameterizations, Climate Dynamics, 54, 4891-4918, 2020.

Tarek, M., Brissette, F. P., and Arsenault, R.: Evaluation of the ERA5 reanalysis as a potential reference dataset for hydrological modelling over North America, Hydrology and Earth System Sciences, 24, 2527-2544, 2020.

Thomas, B. C., and Martin, J. E.: A synoptic climatology and composite analysis of the Alberta clipper, Weather and Forecasting, 22, 315-333, 10.1175/waf982.1, 2007.

Tokay, A., Bashor, P. G., and McDowell, V. L.: Comparison of rain gauge measurements in the mid-Atlantic region, Journal of Hydrometeorology, 11, 553-565, 2010.

Ulbrich, U., Fink, A., Klawa, M., and Pinto, J. G.: Three extreme storms over Europe in December 1999, Weather, 56, 70-80, 2001.

Ulbrich, U., Leckebusch, G. C., and Pinto, J. G.: Extra-tropical cyclones in the present and future climate: a review, Theoretical and Applied Climatology, 96, 117-131, :10.1007/s00704-008-0083-8, 2009.

USGCRP: Impacts, Risks, and Adaptation in the United States: Fourth National Climate Assessment, Volume II, U.S. Global Change Research Program, Washington, DC, USA, 2018.

Varlas, G., Papadopoulos, A., and Katsafados, P.: An analysis of the synoptic and dynamical characteristics of hurricane Sandy (2012), Meteorology and Atmospheric Physics, 131, 443-453, 2019.

https://doi.org/10.5194/nhess-2020-345
Preprint. Discussion started: 11 December 2020

Natural Hazards and Earth System Sciences
Discussions

Villarini, G., Mandapaka, P. V., Krajewski, W. F., and Moore, R. J.: Rainfall and sampling uncertainties: A rain gauge perspective, Journal of Geophysical Research: Atmospheres, 113, doi: 10.1029/2007JD009214, 2008.

Villarini, G., and Krajewski, W. F.: Review of the different sources of uncertainty in single polarization radar-based estimates of rainfall, Surveys in Geophysics, 31, 107-129, 2010.

Vose, R. S., Applequist, S., Bourassa, M. A., Pryor, S. C., Barthelmie, R. J., Blanton, B., Bromirski, P. D., Brooks, H. E., DeGaetano, A. T., and Dole, R. M.: Monitoring and understanding changes in extremes: Extratropical storms, winds, and waves, Bulletin of the American Meteorological Society, 95, 377-386, 2014.

Walz, M. A., Kruschke, T., Rust, H. W., Ulbrich, U., and Leckebusch, G. C.: Quantifying the extremity of windstorms for regions featuring infrequent events, Atmospheric Science Letters, 18, 315-322, 2017.

Walz, M. A., Befort, D. J., Kirchner-Bossi, N. O., Ulbrich, U., and Leckebusch, G. C.: Modelling serial clustering and inter-annual variability of European winter windstorms based on large-scale drivers, International Journal of Climatology, 38, 3044-3057, 2018.

Wan, H., Wang, X. L., and Swail, V. R.: Homogenization and Trend Analysis of Canadian Near-Surface Wind Speeds, Journal of Climate, 23, 1209-1225, 10.1175/2009jcli3200.1, 2010.

Wanik, D., Anagnostou, E., Hartman, B., Frediani, M., and Astitha, M.: Storm outage modeling for an electric distribution network in Northeastern USA, Natural Hazards, 79, 1359-1384, 2015.

Wilks, D. S.: Statistical methods in the atmospheric sciences, International geophysics series, Academic Press. ISBN: 9780123850225, Oxford, UK, 2011. 0123850223

Young, A. M., Skelly, K. T., and Cordeira, J. M.: High-impact hydrologic events and atmospheric rivers in California: An investigation using the NCEI Storm Events Database, Geophysical Research Letters, 44, 3393-3401, 10.1002/2017gl073077, 2017.

Young, G. S., and Kristensen, L.: Surface-layer gusts for aircraft operation, Boundary-Layer Meteorology, 59, 231-242, 10.1007/bf00119814, 1992.

Zielinski, G. A.: A classification scheme for winter storms in the eastern and central United States with an emphasis on nor'easters, Bulletin of the American Meteorological Society, 83, 37-52, 2002.

Zoraghein, H., and O'Neill, B. C.: US State-level Projections of the Spatial Distribution of Population Consistent with Shared Socioeconomic Pathways, Sustainability, 12, 3374, 2020.

Zscheischler, J., Westra, S., Van Den Hurk, B. J., Seneviratne, S. I., Ward, P. J., Pitman, A., AghaKouchak, A., Bresch, D. N., Leonard, M., and Wahl, T.: Future climate risk from compound events, Nature Climate Change, 8, 469-477, 2018.